ANISOTROPIC VISCOUS MODELS OF LARGE DEFORMATION MOHR COULOMB FAILURE

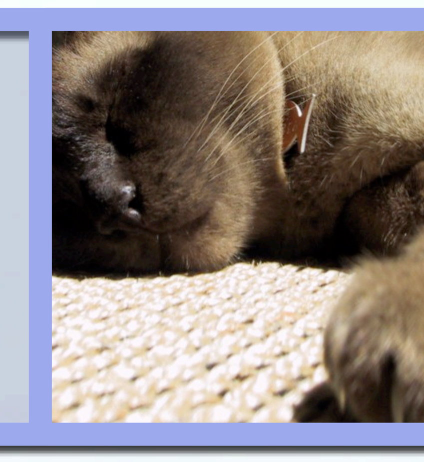

abstract

In mantle convection models it has become common to make use of a modified (pressure sensitive, Boussinesq) von Mises yield criterion to limit the maximum stress the lithosphere can support. This approach allows the viscous, cool thermal boundary layer to deform in a relatively plate-like mode even in a fully Eulerian representation.

In large-scale models with embedded continental crust where the mobile boundary layer represents the oceanic lithosphere, the von Mises yield criterion for the oceans ensures that the continents experience a realistic broad-scale stress regime. In detailed models of crustal deformation it is, however, more appropriate to choose a Mohr-Coulomb yield criterion based upon the idea that frictional slip occurs on whichever one of many randomly oriented planes happens to be favorably oriented with respect to the stress field. As coupled crust/mantle models become more sophisticated it is important to be able to use whichever failure model is appropriate to a given part of the system. We have therefore developed a way to represent Mohr-Coulomb failure within a code which is suited to mantle convection problems coupled to large-scale crustal deformation.

Our approach uses an orthotropic viscous rheology (a different viscosity for pure shear to that for simple shear) to define a prefered plane for slip to occur given the local stress field. The simple-shear viscosity and the deformation can then be iterated to ensure that the yield criterion is always satisfied. We again assume the Boussinesq approximation - neglecting any effect of dilatancy on the stress field. An additional criterion is required to ensure that deformation occurs along the plane aligned with maximum shear strain-rate rather than the perpendicular plane which is formally equivalent in any symmetric formulation.

It is also important to allow strain-weakening of the material. The material should remember both the accumulated failure history and the direction of failure. We have included this capacity in a Lagrangian-Integration-point finite element code and will show a number of examples of extension and compression of a crustal block with a Mohr-Coulomb failure criterion, and comparisons between mantle convection models using the von Mises versus the Mohr-Coulomb yield criteria. The formulation itself is general and applies to 2D and 3D problems, although it is somewhat more complicated to identify the slip plane in 3D.

background

Mantle convection simulations often incorporate a yield criterion to account for the finite strength of the cool lithosphere. On the scale of the lithosphere failure generally occurs through shear on thin fault surfaces — the overburden pressure is sufficiently high to prevent significant opening.

An idealized representation of a fault is an infinitely thin frictional surface which slips when the shear stress (τ_s) overcomes the frictional resistance.

$$\tau_s = \mu\sigma_n + c \tag{1}$$

Where $\tau_s = s_i\sigma_{ij}n_j$, $\sigma_n = n_i\sigma_{ij}n_j$, $\{n_i\}$ is the surface normal and $\{s_i\}$ is the slip direction (See Figure 1b).

On a lithospheric scale where the structure of the fault cannot be resolved, the slip resulting from failure is inherently anisotropic.

Failure model

The Mohr-Coulomb failure model assumes that a fault which develops when an intact material yields occurs at the minimum possible stress for which (1) can be satisfied. In a material with incipient faults of all possible angles (Figure 1a), the ones which can slide at the minimum stress are oriented at $\pm\theta$ to the maximum (here: most compressive) principle stress direction, where

$$\tan 2\theta = \frac{1}{\mu} \tag{2}$$

The slip vector lies in the slip plane in the direction of the minimum principal stress. The two possible failure planes ($\pm\theta$) are entirely equivalent when failure occurs in an intact material.

Anisotropic slip model

Following Mühlhaus et al (Mühlhaus et al., 2002), we define an anisotropic viscous material as a correction to an isotropic viscous part $2\eta D'_{ij}$ of the model by means of the Λ_{ijkl} tensor

$$\sigma_{ij} = 2\eta D'_{ij} - 2(\eta - \eta_s)\Lambda_{ijlm}D'_{lm} - p\delta_{ij} \tag{3}$$

where a prime designates the deviator of the respective quantity, p is the pressure, D_{ij} is the stretching, σ_{ij} is the Cauchy stress and

$$\Lambda_{ijkl} = \frac{1}{2}(n_in_k\delta_{lj} + n_jn_k\delta_{il} + n_in_l\delta_{kj} + n_jn_l\delta_{ik}) - 2n_in_jn_kn_l \tag{4}$$

is the anisotropy tensor. In (3) and (4) the vector n_i is the unit normal of the failure surface given intially by (2). During material deformation, the surface orientation then transforms as

$$\dot{n}_i = n_{i,t} + v_jn_{i,j} = -v_{j,i}n_j \tag{5}$$

where v_i is the velocity vector.

References

L. Moresi, F. Dufour, and H. B. Muhlhaus. A lagrangian integration point finite element method for large deformation modeling of viscoelastic geomaterials. *Journal Of Computational Physics*, 184:476–497, 2003.

H.-B. Mühlhaus, F. Dufour, L. Moresi, and B. Hobbs. A director theory for viscoelastic folding instabilities in multilayered rock. *Int. J. Solids Structures*, 39:3675–3691, 2002.

figure 2

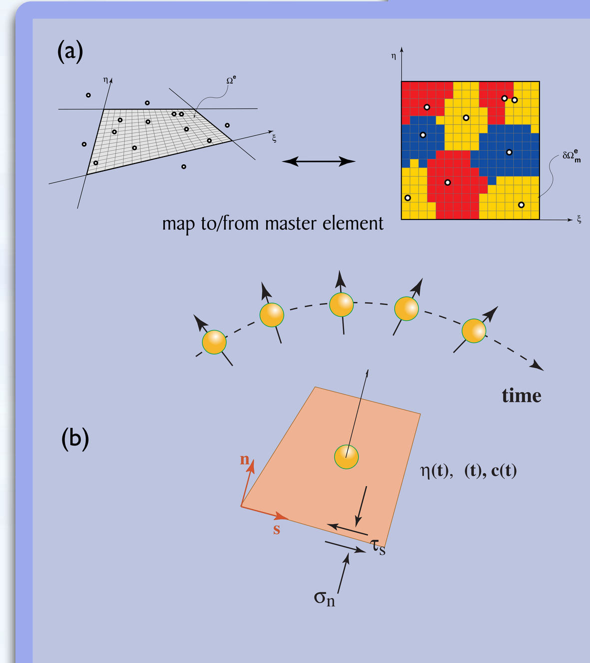

Figure 2 — (a) conceptual picture of the integration sc

figure 1

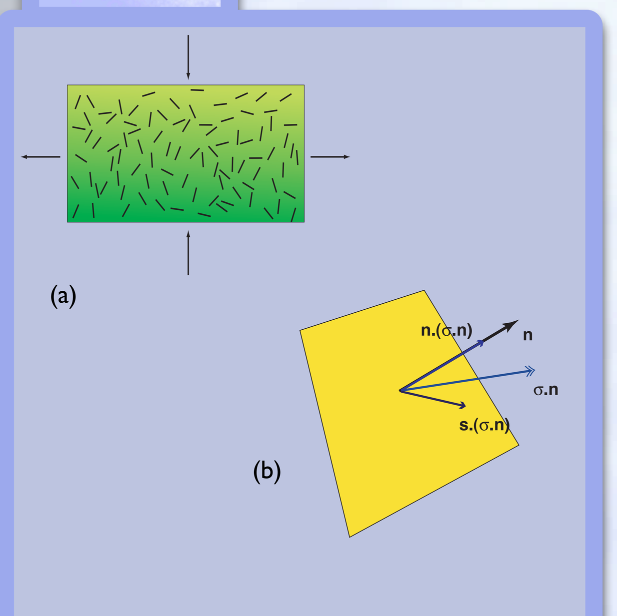

Figure 1 — (a) conceptual picture of a medium with m

figure 3

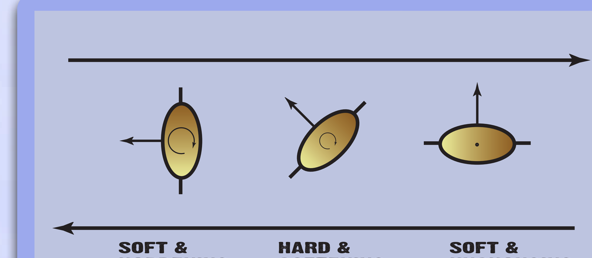

Figure 3 — Director evolution in shear. Due to the syn

computational implementation

The anisotropic viscosity model has been implemented into the Lagrangian integration point finite element code, ELLIPSIS (Moresi et al., 2003).

ELLIPSIS uses a standard mesh to discretize the domain into elements. The shape functions interpolate node points in the mesh in the usual fashion and are used to compute derivatives of nodal variables. Material property variations, and history variables such as failure plane orientation and failure history are stored on integration points which are also material points of the fluid. The problem is formulated through the usual FEM weak form to give an integral equation which is decomposed to a series of element integrals, which, through the usual Galerkin discretization procedure, give element stiffness matrices, $\mathbf{K}^E$:

$$\mathbf{K}^E = \int_{\Omega_E} \mathbf{B}^T(\mathbf{x})\mathbf{C}(\mathbf{x})\mathbf{B}(\mathbf{x})d\Omega \tag{6}$$

we replace the continuous integral by a summation

$$\mathbf{K}^E = \sum_p w_p\mathbf{B}_p^T(\mathbf{x}_p)\mathbf{C}_p(\mathbf{x}_p)\mathbf{B}_p(\mathbf{x}_p) \tag{7}$$

Here the matrix $\mathbf{B}$ consists of the appropriate gradients of interpolation functions which transform nodal point velocity components to strain-rate pseudo-vectors at any points in the element domain. $\mathbf{C}$ the constitutive operator corresponding to (3) is composed of two parts $\mathbf{C} = \mathbf{C}_{iso} + \mathbf{C}_{aniso}$.
In standard finite elements, the positions of the sample points, $\mathbf{x}_p$, and the weighting, w_p are optimized in advance. In our scheme, the $\mathbf{x}_p$'s correspond precisely to the Lagrangian points embedded in the fluid, and w_p must be recalculated at the end of a timestep for the new configuration of particles.

Failure

For a given stress field, σ, the most favorable failure directions are obtained from (2) for each integration point. If the shear stress exceeds the failure criterion in (1), the second viscosity, η_s is set to

$$\eta_s \leftarrow \eta\frac{\mu\sigma_n + c}{\tau_s} \tag{8}$$

which ensures that the stress is returned to the yield surface at this point *assuming no consequent change in the stress field.* This process must then be repeated for all integration points, the stress recalculated, and the whole procedure iterated until changes in the stress field are small.

Failure history

We would like to be able to consider the possibility that the failure of a point is governed by whether the point has failed previously, and that the orientation of previous failure can influence the current failure mode. This means that each integration point should record both a scalar measure of the extent of failure and the preferred orientation of failure (Figure 2b).

In subsequent iterations we consider whether a particle has failed in a previous iteration. If so, then the previous failure plane is tested to see if it will yield allowing for any accumulated weakening of the yield criterion. In the examples shown here, we assume that the plane which has the lowest η_s is the one which will fail first.

hardening v. softening

Due to the symmetry of our anisotropic model there are two equivalent weak orientations — the director is either aligned parallel or perpendicular to the sense of shear. However, only one of these directions (with the director perpendicular to the shear) is stable. When the director is parallel to the shear it rotates in a hardening direction (see equation 5). We therefore need to include as an additional failure criterion the condition that existing failure planes should only fail if they are oriented in the softening direction.

strain history

A measure of the accumulated strain during yield for a given material point is given by the integrating the resolved strain-rate

$$a = \int \frac{\partial u_{\parallel}}{\partial x_{\perp}}dt \tag{9}$$

In our model both the yield strength and the viscosity are strain weakening by the same amount — linearly dependent on the strain measure above normalized by a reference strain, ε_0, and characterized by the ratio of intact strength to strength at ε_0

figure 4

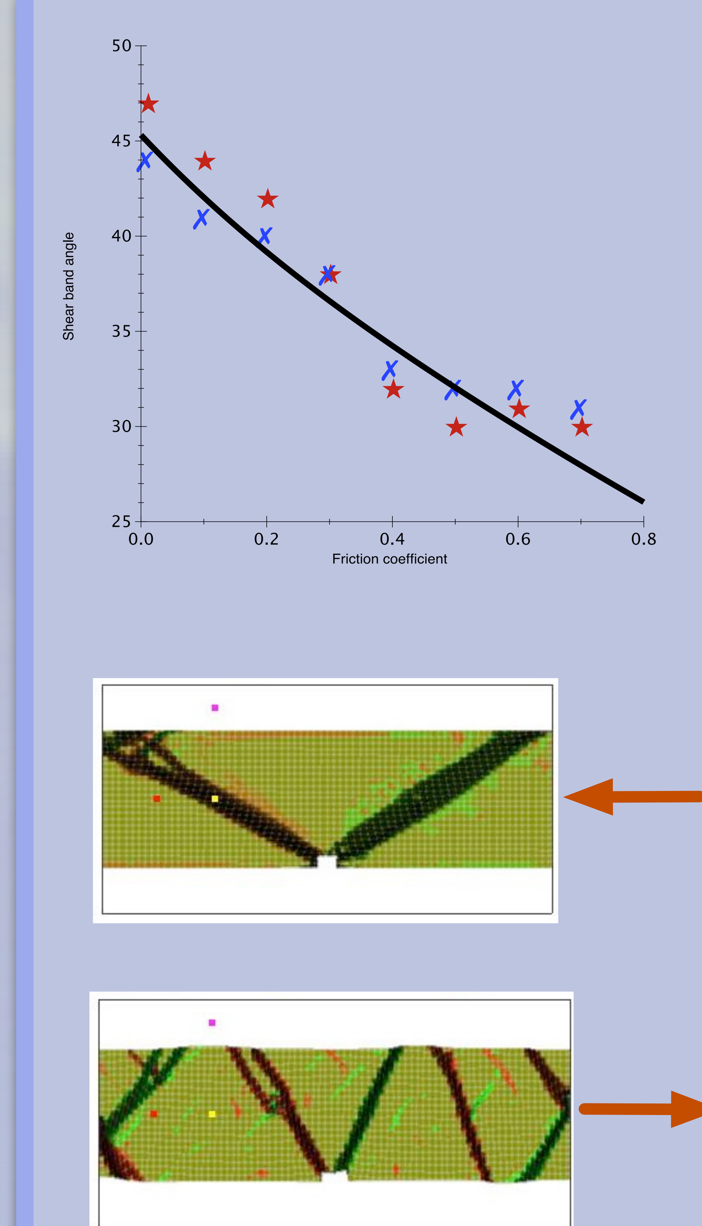

Figure 4 — A simple "benchmark" showing the angle to the vertical

examples

In the examples below the model is applied to a layered system in extension and in compression which is applied as an end velocity boundary condition, $v = \pm 1$. In each case there are three layers: (1) a compressible "air" layer which accomodates the change in volume of the mesh and has a very low viscosity to approximate a free surface boundary on (2) a layer with a viscous / brittle rheology ($\eta = 1.0$, $\mu = 0.4$, $c = 1.5$ in extension, $c = 0.5$ in compression) and strain weakening with $\varepsilon_0 = 0.001$ and strength ratio 0.05. The lower layer is purely viscous, $\eta = 1$

extension

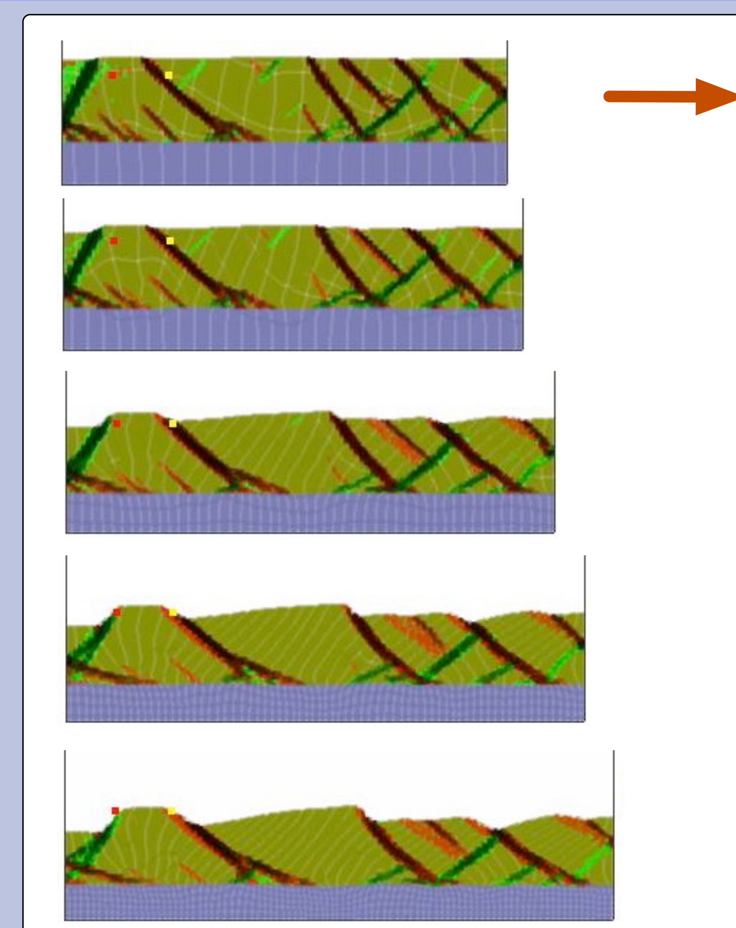

Figure 5— Layer extension: of 6%, 12%, 26%, 40% and 54% horizontal strain

compression

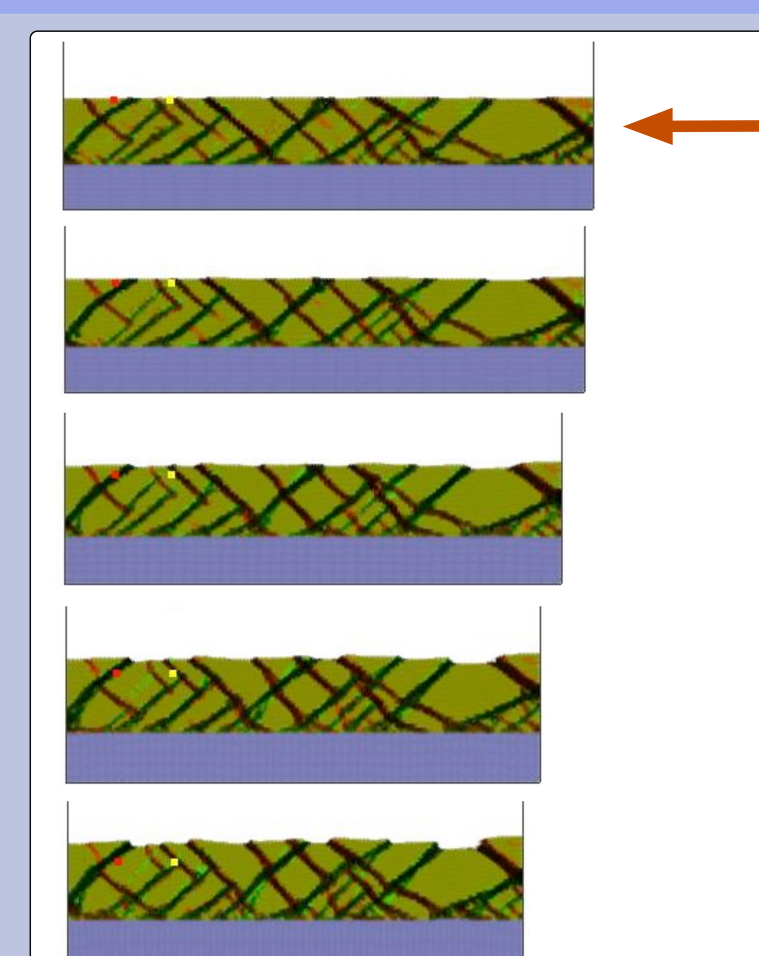

Figure 6 — Layer compression: at 5%, 10%, 20%, 30% and 40% horizontal strain

Louis Moresi, Monash Cluster computing, Monash University, Australia, Louis.Moresi@sci.monash.edu
Hans Mühlhaus, Dept of Earth Sciences, University of Queensland, Australia, muhlhaus@quakes.uq.edu.au